Journal of Drug Delivery Science and Technology 74 (2022) 103493

Contents lists available at ScienceDirect

Journal of Drug Delivery Science and Technology

journal homepage: www.elsevier.com/locate/jddst

The effect of thiol functional groups on bovine serum albumin/chitosan buccal mucoadhesive patches

Ayça Bal-Öztürk [a,b,c,d], Gülşah Torkay [a], Emine Alarçin [e], Zehra Özbaş [f,**,1], Bengi Özkahraman [g,*,1]

[a] Istinye University, Institute of Health Sciences, Department of Stem Cell and Tissue Engineering, 34010, Istanbul, Turkey
[b] Istinye University, Faculty of Pharmacy, Department of Analytical Chemistry, 34010, Istanbul, Turkey
[c] Istinye University, 3D Bioprinting Design & Prototyping R&D Center, 34010, Istanbul, Turkey
[d] Nanotechnology Research and Application Center (SUNUM), Sabancı University, Istanbul, Turkey
[e] Marmara University, Faculty of Pharmacy, Department of Pharmaceutical Technology, 34668, Istanbul, Turkey
[f] Çankırı Karatekin University, Faculty of Engineering, Chemical Engineering Department, 18100, Çankırı, Turkey
[g] Hitit University, Faculty of Engineering, Polymer Materials Engineering Department, 19030, Corum, Turkey

ARTICLE INFO

Keywords:
Thiolated bovine serum albumin
Chitosan
Buccal patch
Ex-vivo mucoadhesion
Triamcinolone acetonide

ABSTRACT

In this research, the effect of thiol functional groups on bovine serum albumin (BSA)/chitosan (Chi) based buccal mucoadhesive patch was investigated. Thiolated BSA (BSA-SH) was prepared via 2-mercaptoethanol. FTIR and ^{1}H NMR results confirmed that BSA-SH was synthesized successfully. The buccal mucoadhesive patches were fabricated by the solvent casting method. Following the structural characterization of BSA/Chi and BSA-SH/Chi buccal patches, the mechanical characterization was performed by tensile tests. The drug release from triamcinolone acetonide (TR) loaded buccal patches was evaluated *in-vitro* in simulated salivary. According to the *ex-vivo* buccal adhesion experiments, the mechanical and mucoadhesion properties of BSA-SH/Chi buccal patch had improved compared to BSA/Chi buccal patch. The total cumulative TR permeated after 12 h was higher for BSA-SH/Chi than BSA/Chi buccal patches. The developed mucoadhesive buccal patches were found to be biocompatible *in vitro*. To conclude, the thiolated BSA-SH/Chi buccal adhesive patch is a promising biomaterial for a satisfied drug delivery, which provides advantages for various oral applications.

1. Introduction

In medical healthcare products, attention has focused on naturally occurring biomaterials of carbohydrate (alginate, chitosan, etc.) and protein (BSA, fibroin, arginin, etc.) structure with nontoxic effects, biocompatible and biodegradable [1–4]. For this reason, biomaterials based on natural polymers suggest different functions to biomimic the extracellular matrix (ECM), cell migration and/or proliferation, tissue regeneration, and water content [5,6]. There are a few studies on BSA in biomaterial applications thus, it has attracted increasing attention in recent years [7–9]. BSA is a water-soluble, globular protein that is plenty and economic due to high purification from bovine blood [3,10]. With the chemical modifications and/or copolymerization of BSA, its properties can be improved and its usability in wider areas can be ensured [3, 11–13]. The chemical structure of thiolated BSA, is significant for its ability to interact with the mucosa for a mucoadhesive character. The thiolated polymers with free thiolated groups in their polymer backbone have good mucoadhesive properties because of the forming intra-disulphide and interdisulphide bridges with the thiolated agent region of the mucosal layer [14,15]. In addition, the high thiolation amount of the polymer backbone provides enhanced mucoadhesive properties [16].

In this study, natural mucoadhesive polysaccharide Chi was used for its capability of increasing the electrostatic interaction between mucin and buccal patches [17,18]. Chi, a cationic polymer, exists *n*-acetyl D-glucosamine and D-glucosamine segments that are analogous to glycosaminoglycan of the ECM [19]. Several researchers have demonstrated the availability of Chi combination in buccal films/patches formulation for oral applications. For example, mucoadhesive buccal

* Corresponding author.
** Corresponding author.
E-mail addresses: zehraozbas@karatekin.edu.tr (Z. Özbaş), bengiozkahraman@hitit.edu.tr (B. Özkahraman).
[1] Equal contribution.

https://doi.org/10.1016/j.jddst.2022.103493
Received 22 March 2022; Received in revised form 21 May 2022; Accepted 6 June 2022
Available online 13 June 2022

films based on Chi-hydroxyethyl cellulose were prepared via solvent casting method to be used treatment of pediatric oral diseases and showed high mucoadhesion behaviour [18]. In addition, Chi-sodium alginate-ethyl cellulose film was developed by solvent-spray drying technique as a buccal drug carrier [20]. There was also an attempt to deliver tenoxicam as a treatment of chronic periodontitis through buccal mucosa by formulating Chi-polyvinyl pyrrolidone buccal films [21]. Another study based on Chi oral mucosa patches was developed by Zheng et al., who prepared triamcinolone acetonide (TR) loaded Chi-Fucoidan patches via chemical crosslinking [22]. TR is an effective topical steroid that is frequently used in patches/film formulations for the treatment of oral cavity problems (ie. aphthous stomatitis, lichen planus, and general inflammatory) [23–26].

To the best of our knowledge, BSA/Chi and BSA-SH/Chi buccal patches were fabricated for the investigation of the thiolated effect on mucoadhesive character for the first time. BSA was thiolated with 2-mercaptoethanol and integrated into the buccal patch formulation to enhance the impact on oral applications. The effect of the thiolation process on the BSA chain was evaluated by structural, mechanical, *ex-vivo* mucoadhesive and *in-vitro* cell culture tests. In addition, *in-vitro* TR release profile was assessed.

2. Experimental

2.1. Materials

BSA, Chi (low molecular weight), glutaraldehyde (Glu) (25% v/v), TR, 3-[4,5-dimethylthiazol-2-yl]-2,5 diphenyltetrazolium bromide (MTT), dimethyl sulfoxide (DMSO), glycerol, HCl, and NaOH were obtained from Sigma-Aldrich. 2-mercaptoethanol and buffered saline pH 6.8 tablet provided from Merck. Buffered saline pH 7.4 tablet was supplied from Sigma-Aldrich. Dulbecco's modified eagle medium (DMEM), penicillin/streptomycin, and fetal bovine serum (FBS) were bought from Biological Industries, Thermo Fisher Scientific, and PAN-Biotech, respectively.

2.2. Synthesis of thiolated BSA polymer (BSA-SH)

The reduced disulfide bond of BSA synthesized by coacervation method according to Martinez et al., protocol [27]. BSA (2.5 g) was dissolved in distilled water (50 mL) at room temperature. Following, pH was adjusted to 8 with 1 M NaOH. For the thiol modification of BSA, 2-mercaptoethanol (60 μL) was added to the reaction medium and kept at 37 °C for 5 h at 100 rpm. Then, pH of the final solution was fixed to 2.5 with HCl (1 M) and the final solution was moved to the dialysis membrane (MWCO: 12–14 kDa). The solution was purified against to HCl solution of pH 3.5 for four days. At the last step, the obtained BSA-SH was lyophilized (Christ Alpha 1–2 LDplus).

2.3. Synthesis of BSA/chitosan (BSA/Chi) and thiolated BSA/chitosan (BSA-SH/Chi) buccal patches

The solvent casting method was used for buccal patch synthesis. Briefly, Chi solution (2% w/v) was prepared with acetic acid (1% v/v) at 30 °C overnight. At the same time, aqueous solutions of BSA (5% w/v) and BSA-SH (5% w/v) were separately prepared at room temperature. The solutions of BSA with Chi and BSA-SH with Chi in the ratio of 1:1 (v/v) were stirred at 25 °C in the presence of glycerol (0.4 g). The Glu solution (25 μL) was added to the polymer syrups for the chemical crosslinking [28]. Then, the syrups of polymer (25 mL) were placed in petri dishes (OD:7.5 cm) and left for 2 days at 25 °C to dry. To prepare drug loaded patches, TR was added into the polymer mixtures of BSA/Chi and BSA-SH/Chi, the patches obtained from the syrup containing TR were labeled as BSA/Chi-TR and BSA-SH/Chi-TR, respectively.

2.4. Characterization

The chemical structure of the BSA, BSA-SH and patches was confirmed by Fourier transform infrared spectroscopy (ATR-FTIR; Bruker). Proton nuclear magnetic resonance (^{1}H NMR; Agilent) spectra were performed in deuterium oxide (D_2O) as a solution at 25 °C, and a frequency of 500 MHz for BSA and BSA-SH.

2.5. Evaluation of swelling and in vitro degradation properties of buccal patches

The swelling capacity in the simulated salivary pH 6.8 medium adsorption into the buccal patches was followed by observing the mass changes for 24 h [29]. Dried buccal patches of the known weight (W_d) were immersed in a swelling medium (20 mL) at 37 °C in the tube. At the equilibrium time, the patches were weighted (W_s) after removing the surface water. The swelling ratio at equilibrium was measured by the following Eq.:

$$Equilibrium\ Swelling\ Ratio = \frac{W_s - W_d}{W_d}$$

The *in-vitro* hydrolytic degradation assay of the fabricated patches was determined in the decreased mass after immersing in the simulated salivary pH 6.8 at 37 °C for set time intervals. Initially, the patches with known weight (W_i) were carried out in the medium to place in a shaking water bath. At specific times, the remaining samples were dried at 40 °C and weighed (W_f). The remaining weight of the buccal patches (hydrolytic degradation) was determined from the following Eq. [30].

$$Remanining\ Weight\ (\%) = \frac{W_i - W_f}{W_f} x\ 100$$

2.6. Mechanical test

The mechanical behaviours of buccal patches were performed by a texture analyzer (Stable Micro Systems). BSA/Chi and BSA-SH/Chi buccal patches samples were cut into 10mm *x* 100 mm (length *x* width) pieces. Buccal patches were fixed between the clamps of the texture analyzer. The initial grip spacing was set at 50 mm. The test was performed at a crosshead speed of 10 mm/min to its breaking point [31]. Tensile-elongation curves and tensile-strength at rupture of the buccal patches were calculated.

2.7. Ex-vivo mucoadhesion test

Cow buccal mucosal tissue was used to consider the mucoadhesive behaviours for the developed BSA/Chi and BSA-SH/Chi buccal patches via the TA.XTplus Texture Analyser. For the fixation of buccal mucosa, a mucoadhesive ring was used. Firstly, the fat regions of the mucosa were removed by a scalpel and a buccal tissue of $2 \times 2\ cm^2$ was attached to the mucoadhesive ring and wetted with pH 6.8 solution (simulated salivary fluid). The samples were fixed with cyanoacrylate glue to the movable platform of the instrument. Then, the platform was raised at 0.5 mm/s speed and came intact with the buccal mucosa for 2 min (applied force 0.5 N). To detach the patches from the mucosal surface, the platform was withdrawn at 0.5 mm/s speed from the mucosal surface. Mucoadhesion force (F_{max}) was identified as the maximum force enforced to entirely separate the patches from the mucosa and work of mucoadhesion (W_{adh}) was determined from the area under the force−distance curve. The test was performed for six patches from each formulation.

2.8. Assay of in-vitro drug release

The TR release behaviour of BSA/Chi-TR and BSA-SH/Chi-TR patch samples were investigated in a release medium of simulated salivary pH 6.8 (10 mL) at 37 °C in a shaking water bath for 2 days. For the

release studies, the buccal patches were trimmed in 1 × 1 mm^2 size. An equivalent volume (3 mL) of fresh buffer solution was exchanged in the experiment at the set time intervals [32]. The obtained calibration curve with a known concentration of TR in pH 6.8 solution was used to convert measured absorbance values into concentration. The indication of the TR absorbance in the aliquots was measured at λ = 242 nm by a UV–Vis Spectrophotometer (Shimadzu UV-1800, JAPAN). The cumulative release (%) was quantified as follows,

$$Cumulative\ release\ (\%) = \left[C_n + \frac{3}{10}\sum C_{n-1}\right] x100$$

where C_n and C_{n-1} are the drug release amount at set time n and n-1, respectively (n = 3).

2.9. Permeation studies

Ex-vivo permeation of TR from BSA/Chi and BSA-SH/Chi buccal patches were investigated across cow buccal mucosa using previously described method with slight modifications [33]. Permeation studies conducted at 37 °C using Franz diffusion cells, with a diffusion area of 3.24 cm^2. The receptor compartment was filled with 25 mL of PBS pH 7.4, bovine buccal mucosa was mounted between the donor and receptor compartments, 5 mL of PBS pH 6.8 was then added to donor compartment, and allowed for 30 min to equilibrate. TR loaded buccal patches were placed onto mucosa, immediately after equilibration time. The receptor compartment was stirred by a magnetic stirrer at 50 rpm. At predetermined time intervals, 3 mL PBS solution was withdrawn from receptor compartment, and replaced with fresh PBS (pH 6.8) to maintain sink condition. The amount of TR in these samples was determined after centrifugation using UV spectrophotometer. Results are reported as amount of drug permeated per unit area (μg/cm^2) as a function of time. The steady-state mass flux (Jss) was calculated as the slope of the cumulative mass-time plotted curve (linear fraction) [34].

2.10. Cell culture

In cell culture studies, NIH/3T3 cell line DMEM consisting of 10% (v/v) FBS and 1% (v/v) penicillin/streptomycin was used as culture media.

2.11. In-vitro cytotoxicity studies

The cytotoxicity of BSA/Chi and BSA-SH/Chi buccal patches was assessed in this work using an indirect MTT colorimetric assay on NIH/3T3 cell lines [1,31,35,36]. Firstly, the patches were sterilized under UV light. Then, the sterilized films were incubated in culture media for 24 h at 37 °C in a 5% CO_2 humidified incubator at an extraction rate of 1 mL per 1 × 1 cm patch. Before use, the culture medium containing the sample extracts was diluted with the equivalent quantity of fresh media and filtered using a syringe-filter having a pore diameter of 0.22 μm. The cells were seeded at a density of 5 × 10^3 cells in 96-well plates. Cultured cells were maintained in a humidified 5% CO_2 incubator at 37 °C overnight. Then, the medium was removed, and the sample extracts were pipetted into the wells. Fresh medium was used as a control. After 24 h incubation at 37 °C in a humidified 5% CO_2 incubator, 10 μL of MTT solution (5 mg/mL in PBS) was added to each well and incubated for another 4 h. Thereafter, the media was removed and replaced with 100 μL of DMSO in each well to dissolve the formazan crystals. After 20 min of a final incubation, absorbance at 570 nm was measured using a microplate reader (BMG LABTECH SPECTROstar® Nano).

2.12. Statistical analysis

Statistical analyses were figured out and given as mean ± standard deviation (SD) by GraphPad Prism Software (V.8.1.0, San Diego, USA). An Unpaired one-tailed *t*-test was used for comparison of between-group data. Differences were examined as statistically significant for P-value < 0.05.

3. Results and discussion

3.1. Characterization of BSA-SH and buccal patches

FTIR-ATR spectrum of BSA, BSA-SH, TR-unloaded and -loaded patches was given in Fig. 1-a-c-d. The main bands of BSA were observed in the FTIR spectrum at 1643 cm^{-1} (amide I), 1520 cm^{-1} (amide II) and 1391 cm^{-1} (amide III). Also, the band observed at 1448 cm^{-1} belongs to the carboxylic group [37]. Since the band of sulfhydryl groups is weak, any new bands were found in the FTIR spectrum of BSA-SH. The amide bands of BSA were also seen in the spectrum of BSA-SH [27]. In the spectrum of BSA/Chi, the bands of BSA have shifted from 1643 cm^{-1} to 1649 cm^{-1} (C═O stretching vibration), and from 1520 cm^{-1} to 1540 cm^{-1} (N–H stretching vibration) due to the electrostatic interaction between cationic CS and anionic BSA (Fig. 1-c) [38,39]. Also, after crosslinking with Glu, a new band at 1037 cm^{-1} was observed because of the COH stretching vibration [40]. Similarly, in the spectrum of BSA-SH/Chi, the bands of BSA-SH has shifted from 1645 cm^{-1} to 1647 cm^{-1} (C═O stretching vibration), and from 1530 cm^{-1} to 1536 cm^{-1} (N–H stretching vibration) due to the electrostatic interaction, and, the new band after crosslinking with Glu was detected at 1033 cm^{-1}. In the spectrum of TR loaded BSA/Chi and BSA-SH/Chi, the absence of new peaks indicated that there is no chemical interaction between the drug and polymer [41,42]. Fig. 1 exhibited the ^{1}H NMR spectra of native BSA (Fig. 1-b) and modified BSA-SH (Fig. 1-d) after the thiolated reaction. The comparison of the ^{1}H NMR spectrum of BSA synthesized with 2-mercaptoethanol supported the proposed structures. For BSA-SH, peaks were shown at 3.80, 2.80 and 2.65 ppm, which was probably due to the protons of thiolether from 2-mercaptoethanol [43].

3.2. Evaluation of swelling and degradation tests

An important factor of ideal patches have capable to swell because contact with oral mucosa occurred to gather moisture and then the patches relatively swelled and got a mucous layer [4]. In addition, favorable swelling behaviour is crucial for uniform drug release and impressive mucoadhesive properties [44]. The swelling characteristic of buccal patches was evaluated in simulated salivary medium at 37 °C and the data illustrated in Fig. 2-a for BSA/Chi and BSA-SH/Chi buccal patches. As shown in Fig. 2-a, the equilibrium swelling ratio of BSA-SH/Chi buccal patch (8.59 ± 1.7 g/g) was 1.4 times higher than that of BSA/Chi buccal patch (6.12 ± 1.1 g/g). This swelling performance of BSA-SH/Chi was due to the added sulfhydryl groups (-SH) in BSA chain [45].

The *in-vitro* hydrolytic degradability of the patches was carried out in the simulated salivary pH 6.8, and their degradability properties were monitored for 14 days. The results were given in Fig. 2-b. Based on these results, BSA-SH/Chi buccal patch displayed a slight degradation profile compared to BSA/Chi buccal patch. This might be explained the content sulfhydryl groups in BSA-SH/Chi buccal patch which water molecules more easily diffuse into polymeric matrix [46]. At the end of 2nd week, weight remaining percentage of BSA/Chi and BSA-SH/Chi buccal patches were found to be ~65% and ~45%, respectively.

3.3. Mechanical and mucoadhesion behaviours of buccal patches

Buccal patches should have mechanical features that enable simply handling and fixing on the buccal mucosa. Notably, their mechanical behaviours have moderate strength potential and certain flexibility to support interaction with the mucosa [47]. This work aimed to fabricate thiolated BSA/Chi patch with enhanced mucoadhesion, mechanical, and controlled release behaviours for the buccal applications. Tensile tests

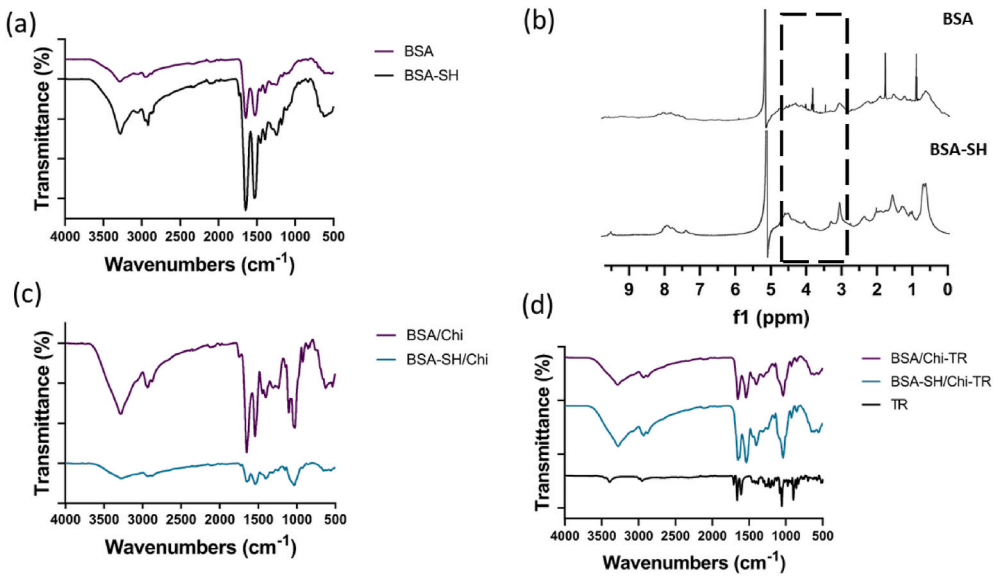

Fig. 1. FTIR (a), and ^{1}H NMR (b) spectra of BSA and BSA-SH. FTIR spectra of BSA/Chi and BSA-SH/Chi (c) buccal patches, and TR, BSA/Chi-TR and BSA-SH/Chi-TR (d) buccal patches.

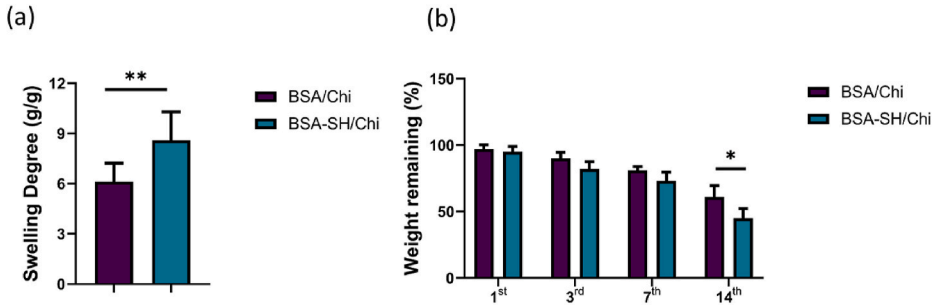

Fig. 2. Water absorption capacity of BSA/Chi and BSA-SH/Chi buccal patches for 24 h (a), and weight remaining (%) of BSA/Chi and BSA-SH/Chi buccal patches after 1st, 3rd, 7th and 14th days (b). Data are given as means ± SD, n = 3. (**: $p < 0.01$, *: $p < 0.05$, ns: $p > 0.05$).

were carried out to designate the effect of thiol units on the BSA backbone on the strength of adhesion. The results are given in Fig. 3-a-b. A highly significant increase in tensile strength was observed BSA-SH/Chi patch (31.36 ± 5.74 MPa) compared to non-thiolated BSA-SH/Chi patch (16.15 ± 3.49 MPa).

Mucoadhesion is defined as the binding potential of the material to the biological tissue [48]. Mucoadhesion is a crucial indicator to evaluate the performance of mucoadhesive buccal patches. In this study, the *ex vivo* mucoadhesion behaviours of BSA/Chi and BSA-SH/Chi patches were performed on cow buccal mucosa. The patches were brought into contact with buccal mucosa and the force and work needed to separate the surfaces were measured. According to the results given in Fig. 3-c-e, immobilization of SH groups on BSA backbone showed that mucoadhesion strength of BSA-SH/Chi buccal patch was half-fold higher (0.64 ± 0.099 N) compared to BSA/Chi buccal patch (0.45 ± 0.10 N). This observation could be attributed to the fact that thiolated-BSA polymer in the gel formulation forms physical and chemical interactions with the cysteine domains of mucin proteins (namely disulfide bonds) on the buccal mucosa [49,50]. In addition, according to the *ex vivo* mucoadhesion studies, BSA-SH/Chi showed a higher work of adhesion (1.36 ± 0.83 N mm) compared with BSA/Chi. (0.92 ± 0.37 N mm) (Fig. 3-e). Consequently, thiol groups on BSA backbone led to the high mucoadhesive potential in BSA-SH/Chi patch.

3.4. Evaluation of in-vitro drug release

The TR release behaviour of BSA/Chi and BSA-SH/Chi patches was found by UV at 242 nm, and the cumulative release (%) amount from these patch formulations versus time was illustrated in Fig. 4. As shown, the releases were increased with time and reached an equilibrium in 24 h. The released amounts were 8.15 mg/g and 9.77 mg/g for BSA/Chi and BSA-SH/Chi, respectively. The higher release value of BSA-SH/Chi patch compared to BSA/Chi polymer was due to the higher swelling amount of BSA-SH/Chi patch [22,23]. In addition, the release mechanism was investigated by applying the drug release data to zero order, first order, Higuchi, and Korsmeyer-Peppas models. The equations, plots, kinetic parameters, and regression coefficients (R^2) were given in Table 1. The release data was fitted most to Korsmeyer-Peppas model, and the diffusion exponent (n) was between 0.45 and 0.89 for both patches which refer to the non-Fickian diffusion of TR molecules through the swollen patches [25].

3.5. Evaluation of ex-vivo permeation

The permeation profiles of TR from BSA/Chi and BSA-SH/Chi buccal patches across cow buccal mucosa were demonstrated in Fig. 5. Data were reported as amount of drug permeated per unit area (μg/cm^2) as a function of time. Lipophilic substances such as TR could result in relatively low permeability due to high tissue retention [51]. However, positively charged Chi could enhance penetration in the presence of

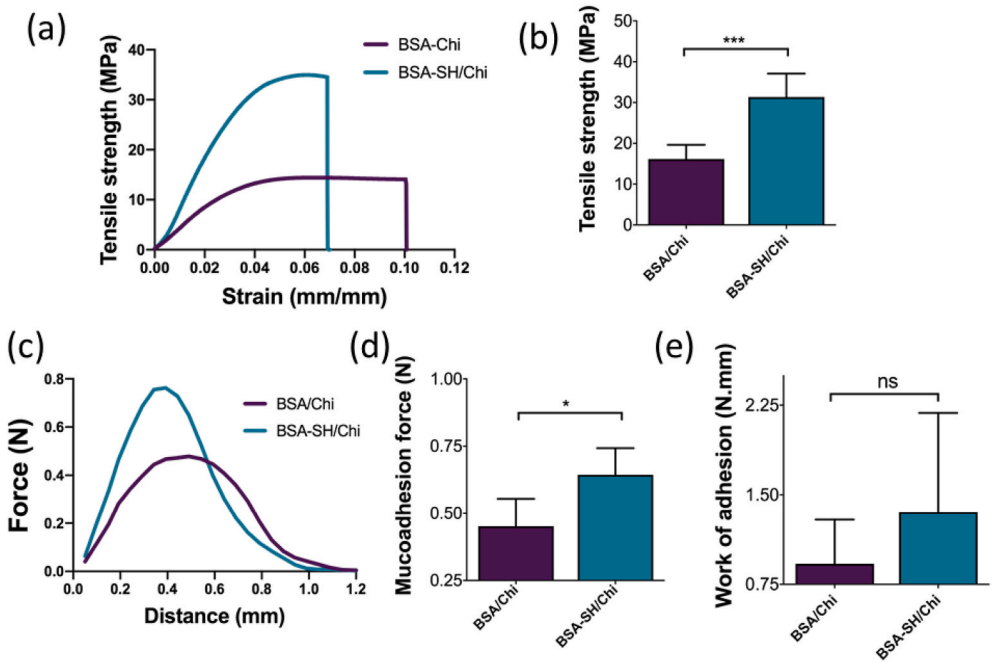

Fig. 3. Mechanical and mucoadhesion properties of BSA/Chi and BSA-SH/Chi buccal patches: (a) Tensile-strain curves, (b) tensile strength, (c) mucoadhesion curves, (d) mucoadhesion force and (e) work of adhesion. Represented data are means ± standard deviation of at least three experiments (***: $p < 0.001$, *: $p < 0.05$, ns: $p > 0.05$).

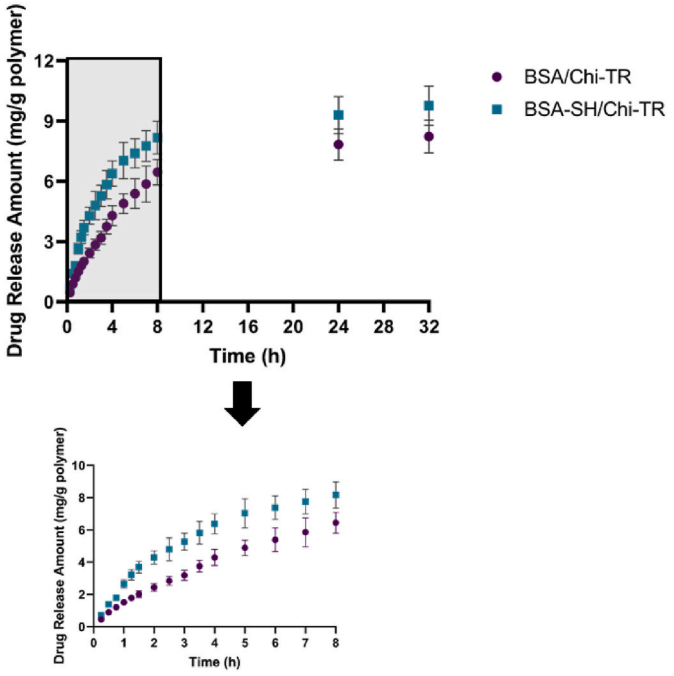

Fig. 4. *In-vitro* cumulative drug release profile of TR from BSA/Chi-TR and BSA-SH/Chi-TR buccal patches in pH 6.8 at 37 °C. Results are presented as means ± SD, n = 3.

mono or stratified epithelia, with or without tight junctions [52]. Herein, the total cumulative TR permeated after 12 h was 62.32 ± 9.87 μg/cm^2 and 76.43 ± 10.45 μg/cm^2 for BSA/Chi and BSA-SH/Chi buccal patches, respectively. In addition, the fluxes of TR were found to be 6.28 ± 1.32 μg cm $^{-2}$ h^{-1} and 7.31 ± 1.4 μg cm^{-2} h^{-1} for BSA/Chi and BSA-SH/Chi buccal patches, respectively. TR permeation from BSA/Chi buccal patches was found to be lower compared to BSA-SH/Chi buccal patches. This could be attributed to relatively slower hydration profile of

Table 1
The defined models and parameters of BSA/Chi-TR and BSA-SH/Chi-TR patches.

Patches	Zero order[a]	First order[a]	Higuchi[a]	Korsmeyer-Peppas[a]
	$q_t = q_0 + k_0.t$	$\ln q_t = \ln q_0 - k_1.t$	$q_t = k_H.\sqrt{t}$	$q_t/q_\infty = k_{KP}.t^n$
	Plot: q_t vs t	Plot: ln q_t vs t	Plot: ln q_t vs $t^{1/2}$	Plot[b]: ln q_t/q_∞ vs ln t
BSA/Chi-TR	k_0: 0.3295 R^2: 0.7271	k_1: 0.0939 R^2: 0.4644	k_H: 0.685 R^2: 0.9284	n: 0.766 k_{KP}: 0.547 R^2: 0.9960
BSA-SH/Chi-TR	k_0: 0.3609 R^2: 0.6098	k_1: 0.0773 R^2: 0.3744	k_H: 0.827 R^2: 0.8614	n: 0.799 k_{KP}: 0.344 R^2: 0.9813

[a] q_t: drug release amount at time t; q_0: initial drug amount in solution (generally zero); k_0, k_1, k_H, and k_{KP}: release constants for zero order, first order, Higuchi and Korsmeyer–Peppas models, respectively; q_t/q_∞: fractional drug release at time t; n: exponent.

[b] 60% of the release data was applied.

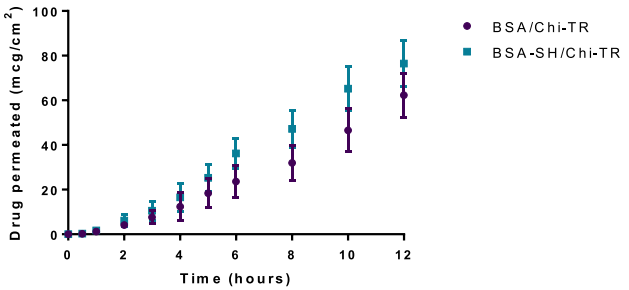

Fig. 5. Ex vivo drug permeation profile of TR from BSA/Chi-TR and BSA-SH/Chi-TR buccal patches across buccal mucosa. Results are presented as means ± SD, n = 3.

BSA/Chi buccal patches. Accordingly, the obtained data demonstrated a favorable correlation with *in vitro* release data, which has a direct effect on available drug amount at absorption site.

3.6. Evaluation of in-vitro cytotoxicity test

Another important attention is the cytotoxicity of the mucoadhesive preparations. Normally, a mucoadhesive system should be non-cytotoxic [53]. In this study, the MTT assay, a rapid colorimetric and quantitative method was used for *in vitro* cytotoxicity studies. The MTT analysis of BSA/Chi, BSA/Chi-TR, BSA-SH/Chi and BSA-SH/Chi-TR patches was performed on the NIH/3T3 cell lines. The results given in Fig. 6 show the cell viability after 24 h treatment with patches extractions. The resultant thiolated patch, BSA-SH/Chi, was found to be not cytotoxic (105.2 ± 12.66% cell viability). Moreover, no visible sign of toxicity was observed with the NIH/3T3 cells after the incubation with BSA-SH/Chi-TR extraction (%83 ± 1.81 cell viability). This means the BSA-SH/Chi and TR loaded form (BSA-SH/Chi-TR) appears to be a safe candidate for mucoadhesive applications.

4. Conclusions

In this research, BSA-Chi and BSA-SH/Chi buccal patches provide comparable mechanical properties, drug release and mucoadhesive performance with each other due to the presence of –SH groups in BSA.

According to our results;

- The FTIR and ^{1}H NMR analysis confirmed that the thiolation reaction of BSA via 2- mercaptoethanol have done successfully.
- In swelling studies of the buccal patches, the presence of –SH groups in BSA-SH/Chi buccal patch played significant role in improving swelling capacity performance.
- The tensile strength of BSA-SH/Chi (31.36 ± 5.74 MPa) was approximately twice that of the BSA/Chi (16.15 ± 3.49 MPa) patch.
- The *ex vivo* mucoadhesion studies revealed that BSA-SH/Chi showed a higher work of adhesion (1.36 ± 0.83 N mm) compared with BSA/Chi (0.92 ± 0.37 N mm).
- The TR release amounts were found to be 8.15 mg/g and 9.77 mg/g for BSA/Chi and BSA-SH/Chi, respectively.
- The total cumulative TR permeated after 12 h was found to be 62.32 ± 9.87 μg/cm^2 and 76.43 ± 10.45 μg/cm^2 for BSA/Chi and BSA-SH/Chi buccal patches, respectively.
- Drug unloaded and loaded BSA/Chi and BSA-SH/Chi buccal patches have no toxic effect on NIH/3T3 cells confirmed by cytocompatibility.

To conclude, the developed BSA-SH/Chi buccal patch could be used as a drug carrier for oral drug delivery, and this biomaterial would be an advantage associated with various applications such as the treatment of oral disease and dental surgery disorders.

Data availability statement

Data available on request from the authors.

Author statement

Ayça Bal Öztürk: Conceptualization, Methodology, Investigation, Resources, Formal analysis, Writing - original draft, Writing - review & editing. Gülşah Torkay: Methodology, Formal analysis. Emine Alarçin: Methodology, Investigation, Resources, Formal analysis, Writing - original draft, Zehra Özbaş: Conceptualization, Methodology, Investigation, Resources, Formal analysis, Writing - original draft, Writing - review & editing. Bengi Özkahraman: Conceptualization, Methodology, Investigation, Resources, Formal analysis, Writing - original draft, Writing - review & editing.

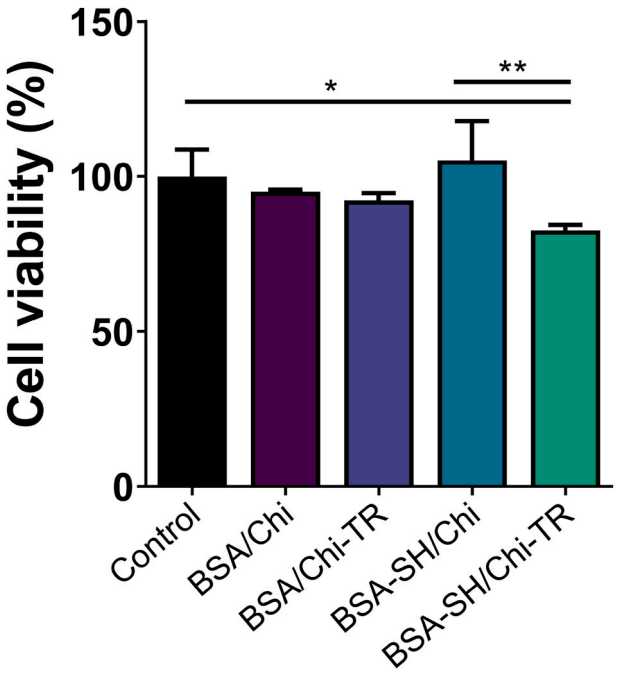

Fig. 6. Cell viability results of BSA/Chi, BSA-SH/Chi and TR-loaded buccal patches were determined by MTT assay. Data are presented as means ± SD, n = 5. (**: $p < 0.01$, *: $p < 0.05$, ns: $p > 0.05$).

Declaration of competing interest

The authors declare that they have no known competing financial interests or personal relationships that could have appeared to influence the work reported in this paper.

Acknowledgement

Gülşah Torkay would like to acknowledge the financial support from the Scientific and Technological Research Council of Turkey (TUBITAK) 2210/A General Domestic Graduate Scholarship Program (App No:1649B022101483).

References

[1] E. Tamahkar, B. Özkahraman, Z. Özbaş, B. Izbudak, F. Yarımcan, F. Boran, A. Bal-Öztürk, Aleo vera-based antibacterial porous sponges for wound dressing applications, J. Porous Mater. 28 (2021) 741–750, https://doi.org/10.1007/s10934-020-01029-1.
[2] L.R. Khoury, I. Popa, Chemical unfolding of protein domains induces shape change in programmed protein hydrogels, Nat. Commun. 10 (2019) 5439, https://doi.org/10.1038/s41467-019-13312-0.
[3] P.T. Smith, B. Narupi, J.H. Tsui, S.C. Millik, R.T. Shafranek, D.H. Kim, A. Nelson, Additive manufacturing of bovine serum albumin-based hydrogels and bioplastics, Biomacromolecules 21 (2020) 484–492, https://doi.org/10.1021/acs.biomac.9b01236.
[4] H. Zheng, B. Zuo, Functional silk fibroin hydrogels: preparation, properties and applications, J. Mater. Chem. B. 9 (2021) 1238–1258, https://doi.org/10.1039/D0TB02099K.
[5] G. Moltalbano, S. Toumpaniari, A. Popov, P. Duan, J. Chen, K. Dalgarno, W. E. Scott III, A.M. Ferreira, Synthesis of bioinspired collagen/alginate/fibrin based hydrogels for soft tissue engineering, Mater. Sci. Eng. C 91 (2018) 236–246, https://doi.org/10.1016/j.msec.2018.04.101.
[6] M. Prasathkumar, S. Sadhasivam, Chitosan/Hyaluronic acid/Alginate and an assorted polymers loaded with honey, plant, and marine compounds for progressive wound healing-Know-how, Int. J. Biol. Macromol. 186 (2021) 656–685, https://doi.org/10.1016/j.ijbiomac.2021.07.067.
[7] H. Yuan, X. Zheng, W. Liu, H. Zhang, J. Shao, J. Yao, C. Mao, J. Hui, D. Fan, A novel bovine serum albumin and sodium alginate hydrogel scaffold doped with hydroxpatite nanowires for cartilage defects repair, Colloids Surf., B 192 (2020), 111041, https://doi.org/10.1016/j.colsurfb.2020.111041.
[8] H. Nosrati, N. Sefidi, A. Sharafi, H. Danafar, H.K. Manjili, Bovine Serum Albumin (BSA) coated iron oxide magnetic nanoparticles as biocompatible carriers for

curcumin-anticancer drug, Bioorg. Chem. 76 (2018) 501–509, https://doi.org/10.1016/j.bioorg.2017.12.033.
[9] H. Nosrati, A. Rakhshbahar, M. Salehiabar, S. Afroogh, H.K. Manjili, H. Danafar, S. Davaran, Bovine serum albumin: an efficient biomacromolecule nanocarrier for improving the therapeutic efficacy of chrysin, J. Mol. Liq. 271 (2018) 639–646, https://doi.org/10.1016/j.molliq.2018.06.066.
[10] M. Gharbavi, H.K. Manjili, J. Amani, A. Sharafi, In vivo and in vitro biocompatibility study of novel microemulsion hybridized with bovine serum albümin as nanocarrier for drug delivery, Heliyon 5 (2019), e01858, https://doi.org/10.1016/j.heliyon.2019.e01858.
[11] F. Iemma, U.G. Spizzirri, F. Puoci, P.R. Muzzalupo, S. Trombino, R. Cassano, S. Leta, N. Picci, pH-Sensitive hydrogels based on bovine serum albumin for oral drug delivery, Int. J. Pharm. 312 (2006) 151–157, https://doi.org/10.1016/j.ijpharm.2006.01.010.
[12] D. Tada, T. Tanabe, A. Tachibana, K. Yamauchi, Drug release from hydrogel containing albumin as crosslinker, J. Biosci. Bioeng. 100 (5) (2005) 551–555, https://doi.org/10.1263/jbb.100.551.
[13] M.A. Silva, S. Lenton, M. Hughes, D.J. Brockwell, L. Dougan, Assessing the potential of folded globular polyproteins as hydrogel building blocks, Biomacromolecules 18 (2017) 636–646, https://doi.org/10.1021/acs.biomac.6b01877.
[14] K. Netsomboon, A. Jalil, F. Laffleur, A. Hupfauf, R. Gust, A. Bernkop-Schnürch, Thiolated chitosan: are Cys-Cys ligands key to the next generation? Carbohydr. Polym. 242 (2020), 116395 https://doi.org/10.1016/j.carbpol.2020.116395.
[15] S. Summonte, G.F. Racaniello, A. Lopedota, N. Denora, A. Bernkop-Schnürch, Thiolated polymeric hydrogels for biomedical application: cross-linking mechanisms, J. Contr. Release 330 (2021) 470–482, https://doi.org/10.1016/j.jconrel.2020.12.037.
[16] M.H. Asim, I. Nazir, A. Jalil, B. Matuszczak, A. Bernkop-Schnürch, Tetradeca-thiolated cyclodextrins: highly mucoadhesive and in-situ gelling oligomers with prolonged mucosal adhesion, Int. J. Pharm. 577 (2020), 119040, https://doi.org/10.1016/j.ijpharm.2020.119040.
[17] A. Göbel, J.B. Silva, M. Cook, J. Breitkreutz, Development of buccal film formulation and their mucoadhesive performance in biomimetic models, Int. J. Pharm. 610 (2020), 121233, https://doi.org/10.1016/j.ijpharm.2021.121233.
[18] D. Abouhussein, M.A.E. Nabarawi, S.H. Shalaby, A.A. El-Bary, Cetylpyridinium chloride chitosan blended mucoadhesive buccal films for treatment of pediatric oral diseases, J. Drug Deliv. Sci. Technol. 57 (2020), 101676, https://doi.org/10.1016/j.jddst.2020.101676.
[19] A.S. Soubhagya, A. Moorthi, M. Prabaharan, Preparation and characterization of chitosan/pectin/ZnO porous films for wound healing, Int. J. Biol. Macromol. 157 (2020) 135–145, https://doi.org/10.1016/j.ijbiomac.2020.04.156.
[20] S. Wang, Z. Gao, L. Liu, M. Li, A. Zuo, J. Guo, Preparation, in vitro and in vivo evaluation of chitosan-sodium alginate-ethyl cellulose polyelectrolyte film as novel buccal mucosal delivery vehicle, Eur. J. Pharmaceut. Sci. 168 (2022), 106085, https://doi.org/10.1016/j.ejps.2021.106085.
[21] L.Y. Ashri, , A.E.S.F.A.E. Ela, M.A. Ibrahim, D.H. Alshora, M.J. Naguib, Optimization and evaluation of chitosan buccal films tenoxicam for treating chronic periodontitis: in vitro and in vivo studies, J. Drug Deliv. Sci. Technol. 57 (2020), 101720, https://doi.org/10.1016/j.jddst.2020.101720.
[22] W. Zheng, Y. Hao, D. Wang, H. Huang, F. Guo, Z. Sun, P. Shen, K. Sui, C. Yuan, Q. Zhou, Preparation of triamcinolone acetonide-loaded chitosan/fucoidan hydrogel and its potential application as an oral mucosa patch, Carbohydr. Polym. 272 (2021), 118493, https://doi.org/10.1016/j.carbpol.2021.118493.
[23] F.P. Fernandes, A.C. Fortes, C.S.G. Fonseca, J. Breitkreutz, H.G. Ferraz, Manufacture and characterization of mucoadhesive buccal films based on pectin and gellan gum containing triamcinolone acetonide, Int. J. Polym. Sci. (2018), https://doi.org/10.1155/2018/2403802. Article ID: 2403802.
[24] H.S. Seon-Woo, H.J. Kim, J.Y. Roh, J.H. Park, Dissolving microneedle systems for the oral mucosal delivery of triamcinolone acetonide to treat aphthous stomatitis, Macromol. Res. 27 (2019) 282–289, https://doi.org/10.1007/s13233-019-7031-6.
[25] Z. Özbaş, B. Özkahraman, Z.P. Akgüner, A. Bal-Öztürk, Evaluation of modified pectin/alginate buccal patches with enhanced mucoadhesive properties for drug release systems: in-vitro and ex-vivo study, J. Drug Deliv. Sci. Technol. 67 (2022), 102991, https://doi.org/10.1016/j.jddst.2021.102991.
[26] B. Özkahraman, Z. Özbaş, G. Yaşayan, Z.P. Akgüner, F. Yarımcan, E. Alarçin, A. Bal-Öztürk, Development of mucoadhesive modified kappa-carrageenan/pectin patches for controlled delivery of drug in the buccal cavity, J. Biomed. Mater. Res. (2021), https://doi.org/10.1002/jbm.b.34958.
[27] A. Martinez, I. Iglesias, R. Lozano, J.M. Teijon, M.D. Blanco, Synthesis and characterization of thiolated alginate-albumin nanoparticles stabilized by disulfide bonds. Evaluation as drug delivery systems, Carbohydr. Polym. 83 (2011) 1311–1321, https://doi.org/10.1016/j.carbpol.2010.09.038.
[28] H. Nosrati, M. Salehiabar, H.K. Manjili, H. Danafar, S. Davaran, Preparation of magnetic albumin nanoparticles via asimple an done-pot desolvation and co-precipitation method for medical pharmaceutical applications, Int. J. Biol. Macromol. 108 (2018) 909–915, https://doi.org/10.1016/j.ijbiomac.2017.10.180.
[29] B. Özkahraman, Z. Özbaş, G. Bayrak, E. Tamahkar, I. Perçin, A. Kılıç-Süloğlu, F. Boran, Characterization and Antibacterial activity of gelatin-gellan gum bilayer wound dressing, Int. J. Polym. Mater. (2021), https://doi.org/10.1080/00914037.2021.1960341.
[30] B. Özkahraman, E. Tamahkar, N. İdil, A. Kılıç Süloğlu, I. Perçin, Evaluation of hyaluronic acid nanoparticle embedded chitosan-gelatin hydrogels for antibiotics release, Drug Dev. Res. 82 (2) (2021) 241–250, https://doi.org/10.1002/ddr.21747.
[31] N. Özen, Z. Özbaş, B. İzbudak, S. Emik, B. Özkahraman, A. Bal-Öztürk, Boric acid-impregnated silk fibroin/gelatin/hyaluronic acid-based films for improving the wound healing process, J. Appl. Polym. Sci. 139 (9) (2022), 51715, https://doi.org/10.1002/app.51715.
[32] H. Mert, B. Özkahraman, H. Damar, A novel wound dressing material: pullulan grafted copolymer hydrogel via UV copolymerization and crosslinking, J. Drug Deliv. Sci. Technol. 60 (2020), 101962, https://doi.org/10.1016/j.jddst.2020.101962.
[33] M. Gajdošová, D. Vetchy, J. Muselik, J. Gajdziok, J. Jurica, M. Vetcha, K. Houptman, V. Jekl, Bilayer mucoadhesive buccal films with prolonged release of ciclopirox olamine for the treatment of oral candidiasis: in vitro development, ex vivo permeation testing, pharmacokinetic and efficacy study in rabbits, Int. J. Pharm. 592 (2021), 120086, https://doi.org/10.1016/j.ijpharm.2020.120086.
[34] G.K. Eleftheriadis, C. Ritzoulis, N. Bouropoulos, D. Tzetzis, D.A. Andreadis, J. Boetker, J. Rantanen, D.G. Fatouros, Unidirectional drug release from 3D printed mucoadhesive buccal films using FDM technology: in vitro and ex vivo evaluation, Eur. J. Pharm. Biopharm. 144 (2019) 180–192, https://doi.org/10.1016/j.ejpb.2019.09.018.
[35] A. Bal-Öztürk, Z.P. Akgüner, Silk fibroin/polyvinly alcohol based drug carrier wound dressings, SDU J. Nat. Appl. Sci. 24 (1) (2020) 25–34.
[36] G. Yaşayan, G. Karaca, Z.P. Akgüner, A. Bal-Öztürk, Chitosan/collagen composite films as wound dressing encapsulating allantoin and lidocaine hydrochloride, Int. J. Polym. Mater. 70 (9) (2021) 623–635, https://doi.org/10.1080/00914037.2020.1740993.
[37] M.M. Rashad, N.M. El-Kemary, S. Amer, M. El-Kemary, Bovine serum albumin/chitosan-nanoparticle bio-complex; spectroscopic study and in vivo toxicological – hypersensitivity evaluation, Spectrochim. Acta. A. Biomol. Spectrosc. 253 (2021), 119582, https://doi.org/10.1016/j.saa.2021.119582.
[38] M.H. Kafshgari, M. Khorram, M. Khodadoost, S. Khavari, Reinforcement of chitosan nanoparticles obtained by an ionic cross-linking process, Iran, Polym. J. 20 (5) (2011) 445–456.
[39] X. Gao, N. Liu, Z. Wang, J. Gao, H. Zhang, M. Li, Y. Du, X. Gao, A. Zheng, Development and optimization of chitosan nanoparticle-based intranasal vaccine carrier, Molecules 27 (2022) 204, https://doi.org/10.3390/molecules27010204.
[40] A.R. Raut, S.R. Khairkar, Study of chitosan crosslinked with glutaraldeyde as biocomposite material, World J. Pharmaceut. Res. 3 (9) (2014) 523–532.
[41] J.S. Ahn, H.K. Choi, M.K. Chun, J.M. Ryu, J.H. Jung, Y.U. Kim, C.S. Cho, Release of triamcinolone acetonide from mucoadhesive polymer composed of chitosan and poly(acrylic acid) in vitro, Biomaterials 23 (2002) 1411–1416, https://doi.org/10.1016/S0142-9612(01)00261-7.
[42] S. Payab, S. Davaran, A. Tanhaei, B. Fayyazi, A. Jahangiri, A. Farzaneh, K. Adibkia, Triamcinolone acetonide–eudragit® RS100 nanofibers and nanobeads: morphological and physicochemical characterization, artif cells nanomed, Biotechnol. 44 (1) (2016) 362–369, https://doi.org/10.3109/21691401.2014.953250.
[43] W. Wu, X. Zeng, H. Li, X. Lai, H. Xie, Synthesis and antioxidative properties in natural rubber of novel macromolecular hindered phenol antioxidants containing thioether and urethane groups, Polym. Degrad. 111 (2015) 232–238, https://doi.org/10.1016/j.polymdegradstab.2014.12.001.
[44] V.M. Patel, B.G. Prajapati, M.M. Patel, Formulation, evaluation, and comparison of bilayered and multilayered mucoadhesive buccal devices of propanolol hydrochloride, AAPS PharmSciTech 8 (1) (2007), https://doi.org/10.1208/pt0801022. Article 22.
[45] A. Jalil, M.H. Asim, N.M.N. Le, F. Laffleur, B. Matuszczak, M. Tribus, A. Bernkop-Schnürch, S-protected gellan gum: decisive approach towards mucoadhesive antimicrobial vaginal films, Int. J. Biol. Macromol. 130 (2019) 148–157, https://doi.org/10.1016/j.ijbiomac.2019.02.092.
[46] M. Akrami-Hasan-Kohal, M. Ghorbani, F. Mahmoodzadeh, B. Nikzad, Development of reinforced aldehyde-modified kappa-carrageenan/gelatin film by incorporation of halloysite nanotubes for biomedical applications, Int. J. Biol. Macromol. 160 (2020) 669–676, https://doi.org/10.1016/j.ijbiomac.2020.05.222.
[47] J.F. Alopaeus, M. Helfritzsch, T. Gutowski, R. Scherliess, A. Almeida, B. Sarmento, N. Skalko-Basnet, I. Tho, Mucoadhesive buccal films based on a grafted co-polymer-A mucin-retentive hydrogel scaffold, Eur. J. Pharmaceut. Sci. 142 (2020), 105142, https://doi.org/10.1016/j.ejps.2019.105142.
[48] E. Cevher, D. Sensoy, M.A.M. Taha, A. Araman, Effect of thiolated polymers to textural and mucoadhesive properties of vaginal gel formulations prepared with polycarbophil and chitosan, AAPS PharmSciTech 9 (2008) 953–965, https://doi.org/10.1208/s12249-008-9132-y.
[49] B.A. Szilagyi, B. Gyarmati, G. Horvat, A. Laki, M. Bugai-Szucs, E. Csanyi, G. Sandri, M.C. Bonferoni, A. Szilagyi, The effect of thiol content on the gelation and mucoadhesion of thiolated poly(aspartic acid), Polym. Int. 66 (11) (2017) 1538–1545, https://doi.org/10.1002/pi.5411.
[50] M.S. Hosseini, B. Kamali, M.R. Nabid, Multilayered mucoadhesive hydrogel films based on Ocimum basilicum seed mucilage/thiolated alginated/dopamine-modified hyaluronic acid and PDA coating for sublingual administration of nystatin, Int. J. Biol. Macromol. 203 (2022) 93–104, https://doi.org/10.1016/j.ijbiomac.2022.01.031.

[51] T. Caon, C.M.O. Simões, Effect of freezing and type of mucosa on ex vivo drug permeability parameters, AAPS PharmSciTech 12 (2) (2011) 587–592, https://doi.org/10.1208/s12249-011-9621-2.

[52] C. Padula, I. Telò, A. Di Ianni, S. Pescina, S. Nicoli, P. Santi, Microemulsion containing triamcinolone acetonide for buccal administration, Eur. J. Pharmaceut. Sci. 115 (2018) 233–239, https://doi.org/10.1016/j.ejps.2018.01.031.

[53] K. Kim, K. Kim, J.H. Ryu, H. Lee, Chitosan-catechol: a polymer with long-lasting mucoadhesive properties, Biomaterials 52 (2015) 161–170, https://doi.org/10.1016/j.biomaterials.2015.02.010.